Electronic Supplementary Material (ESI) for Green Chemistry.

Supporting Information

Integrating electrocatalytic seawater splitting and biomass upgrading via bifunctional nickel cobalt phosphide nanorods

Yunyi Yang[a], Ren Zou[a], Jianyun Gan[a], Yujia Wei[a], Zhongxin Chen[c], Xuehui Li[a], Shimelis Admassie[d], Yunpeng Liu[b,*], and Xinwen Peng[a,*]

[a] *State Key Laboratory of Pulp and Paper Engineering, South China University of Technology, Guangzhou 510641, Guangdong, China*

[b] *School of Materials Science and Hydrogen Energy, Foshan University, Foshan 528231, Guangdong, China*

[c] *School of Science and Engineering, The Chinese University of Hong Kong, Shenzhen 518172, Guangdong, China.*

[d] *School of Materials Science and Engineering, South China University of Technology, Guangzhou 510640, Guangdong, China*

* Corresponding author. E-mail: fexwpeng@scut.edu.cn (X. Peng)

* Corresponding author. E-mail: l.yunpeng@fosu.edu.cn (Y. Liu)

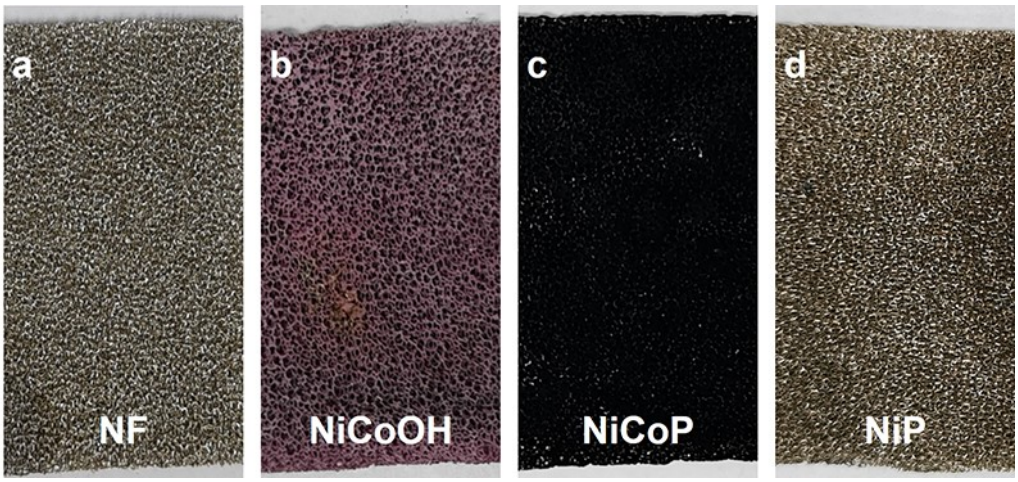

Fig. S1. (a) Digital photos of Ni foam, NiCoOH, NiCoP and NiP.

NiCoOH precursor, NiCoP and NiP are silver, purple, black and dark silver, respectively.

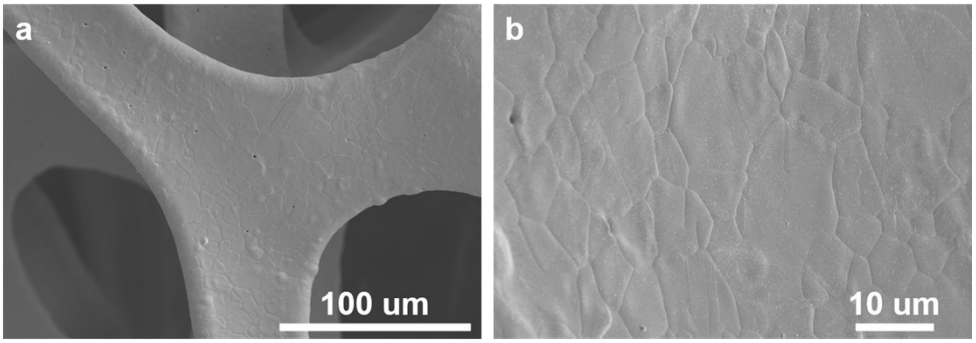

Fig. S2. SEM images of Ni foam.

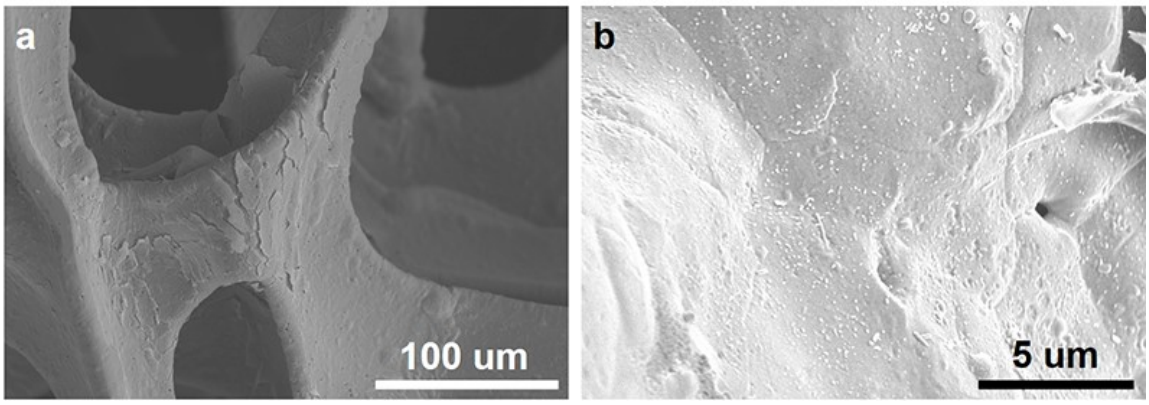

Fig. S3. SEM images of NiP.

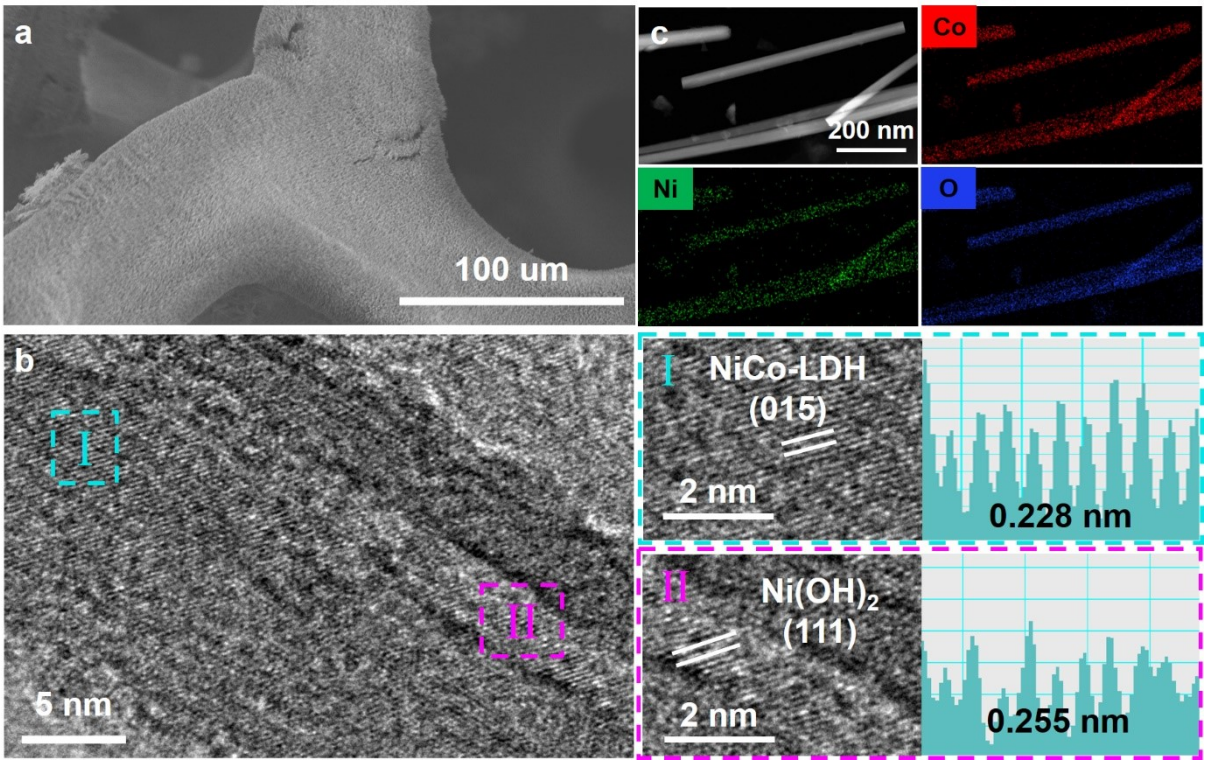

Fig. S4. (a) TEM, (b) HRTEM and (c) elemental mappings images of NiCoOH.

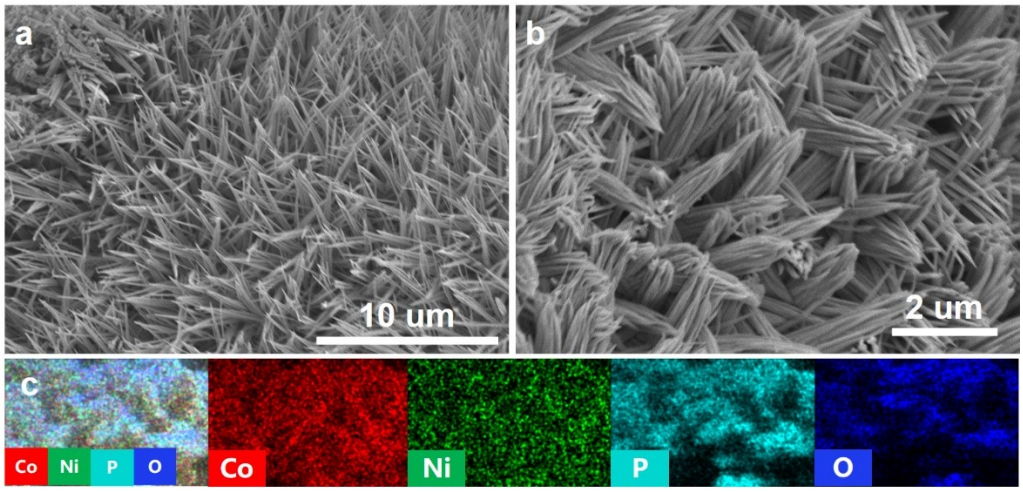

Fig. S5. (a-b) SEM images and (c) elemental mappings of NiCoP.

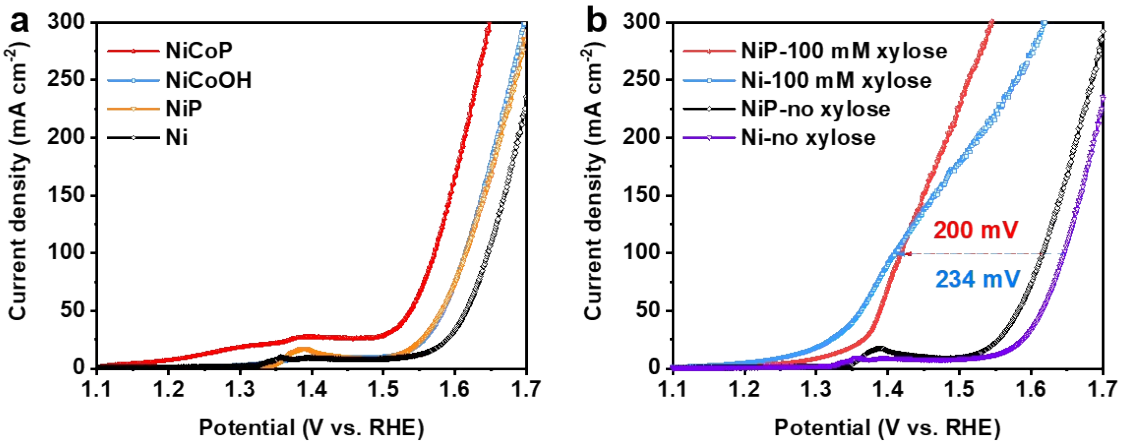

Fig. S6. (a) LSV curves of different electrocatalysts in 1.0 M KOH. (b) LSV curves of NiP and NF with and without 100 mM xylose.

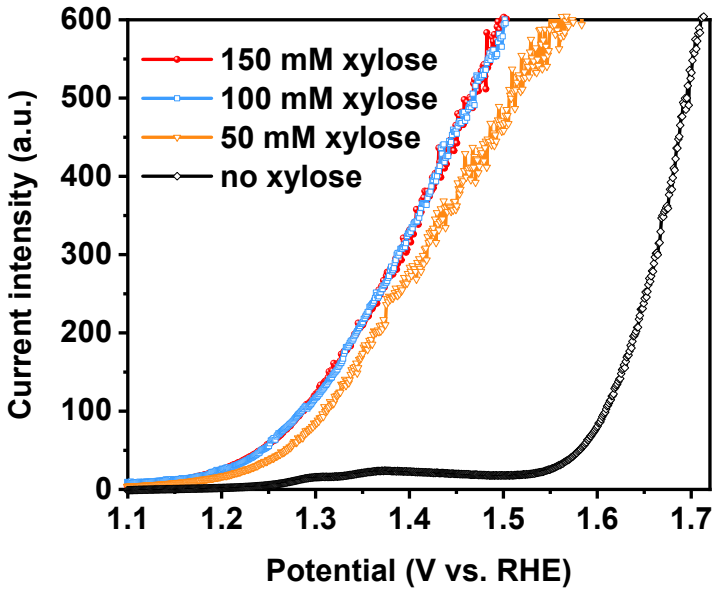

Fig. S7. LSV curves of NiCoP in 1.0 M KOH with different concentrations of xylose.

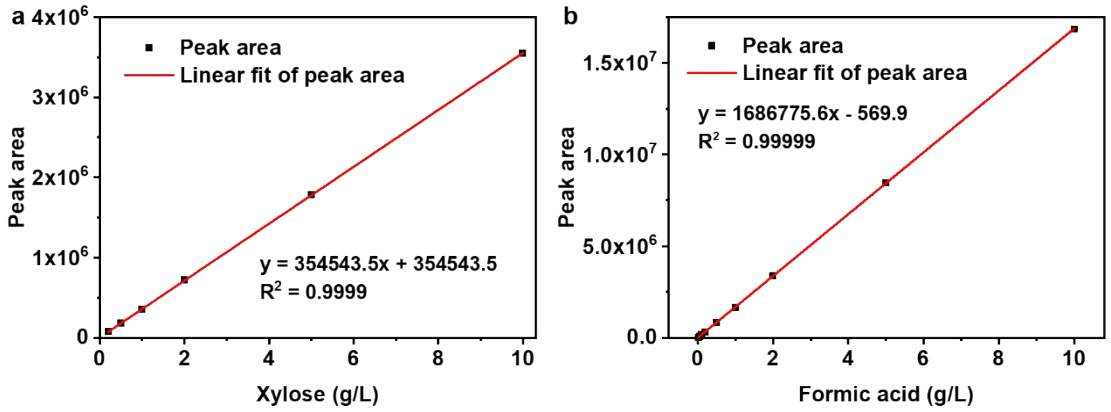

Fig. S8. The calibration curve of xylose (a) and formic acid (b) established with the external standards.

Calibration curves generated by regression of nominal concentrations against peak area were used to determine the concentrations of the products.

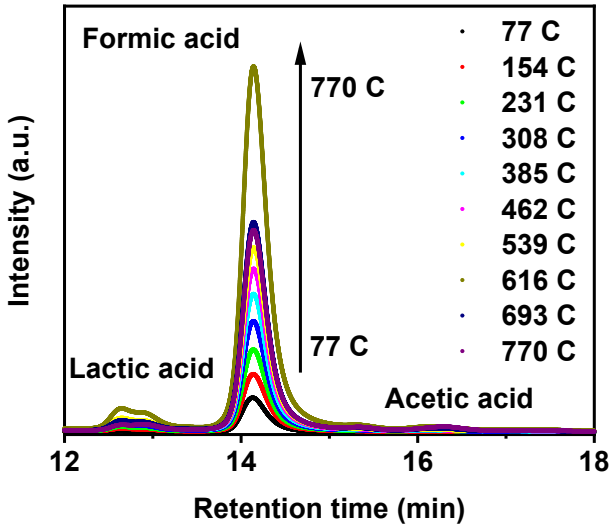

Fig. S9. HPLC traces of XOR after passing different charges at 1.52 V (*vs.* RHE).

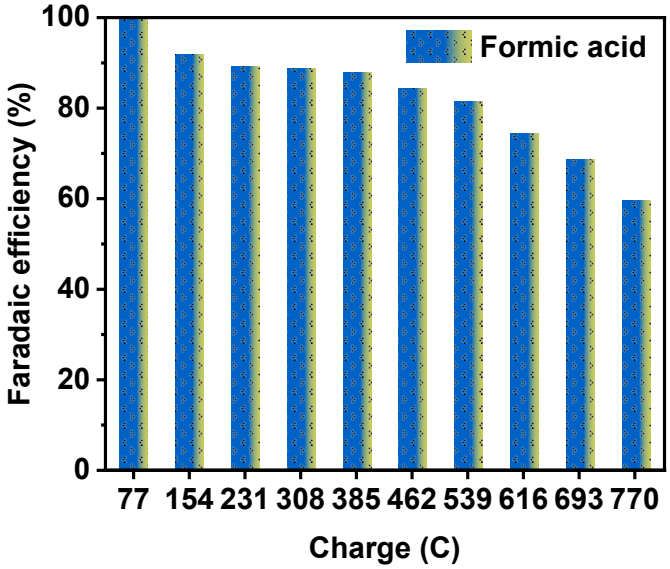

Fig. S10. The Faradaic efficiency of FA from xylose after passing different charges at 1.52 V (*vs*. RHE) in 1.0 M KOH.

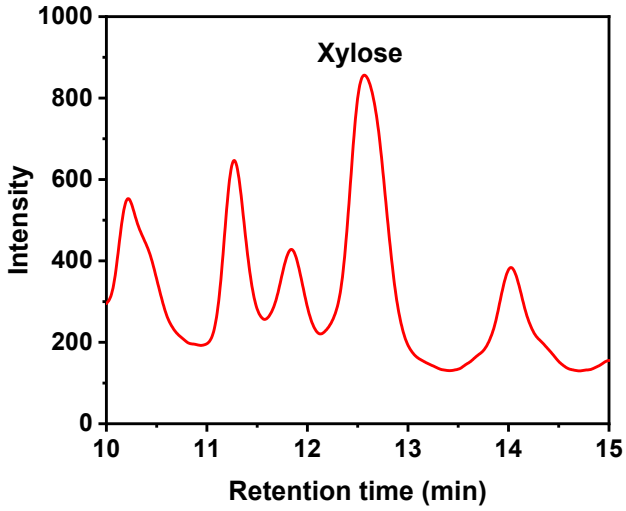

Fig. S11. HPLC traces of XOR after passing 693 C charges at 1.52 V (*vs.* RHE).

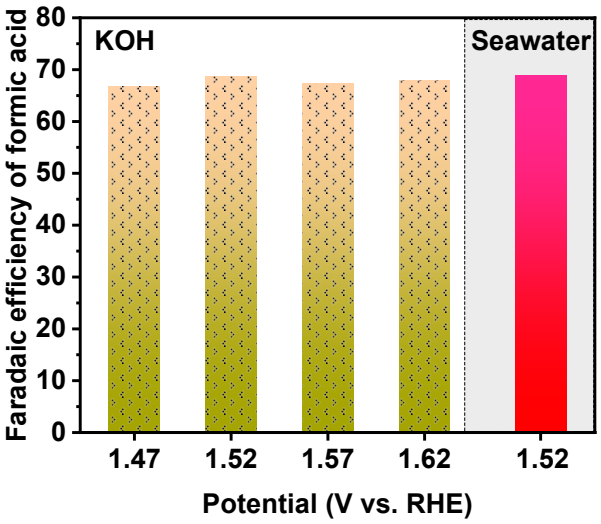

Fig. S12. The Faradaic efficiency of FA in 8 mL of 100 mM xylose at different potentials in 1.0 M KOH.

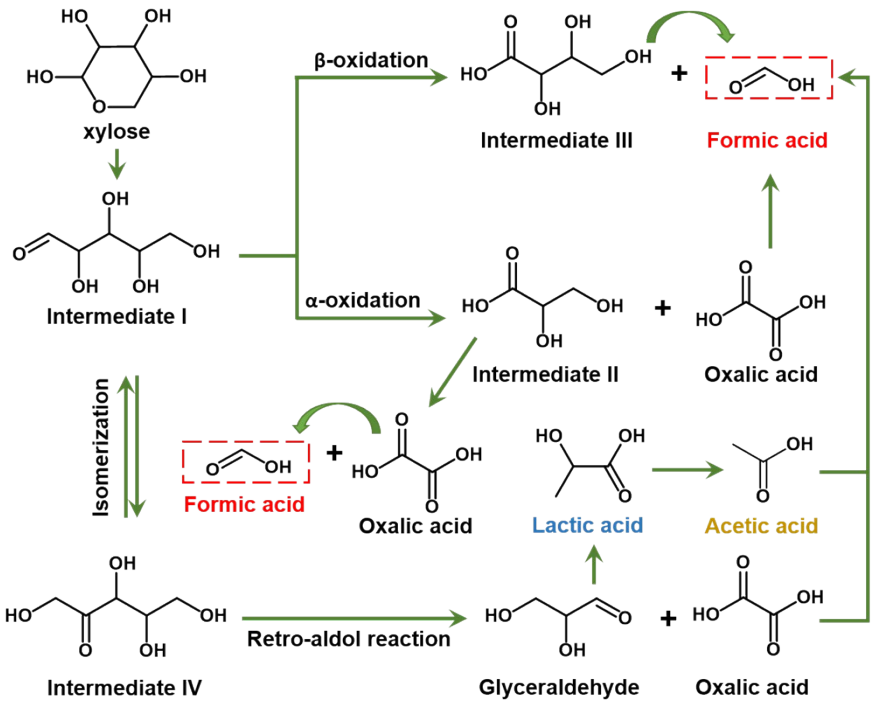

Fig. S13. The possible pathway of xylose electrooxidation to formic acid, lactic acid and acetic acid.

The possible pathways of electrooxidation of xylose to formic acid are proposed in the below figure (Fig. S13). Under the condition of 1.0 M KOH, the ring-open reaction occurs on annular xylose molecules to form the intermediate I. Then the intermediate I is oxidized to intermediate II and oxalic acid by α-oxidation, as well as intermediate III and formic acid by β-oxidation. The intermediate II is converted to oxalic acid and formic acid, while the intermediate III is converted to formic acid. The above oxalic acid is further oxidized to formic acid. Additionally, isomerization may also occur on the intermediate I to from the intermediate IV, which is oxidized to glyceraldehyde and oxalic acid by Retro-aldol reaction. Glyceraldehyde transforms into lactic acid and the lactic acid is oxidized to acetic acid. Finally, the produced oxalic acid and acetic acid are converted to formic acid.

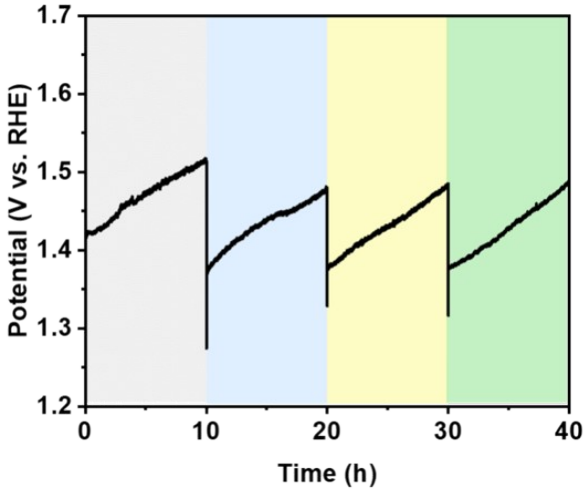

Fig. S14. Consecutive four runs of XOR at a constant current of 50 mA cm^{-2} with the intermittent addition of 100 mM xylose.

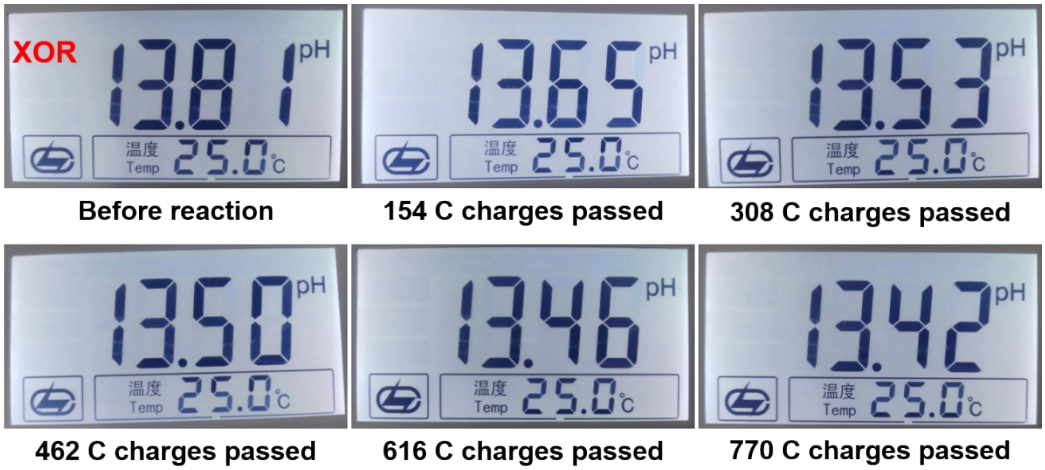

Fig. S15. The change of pH value during XOR.

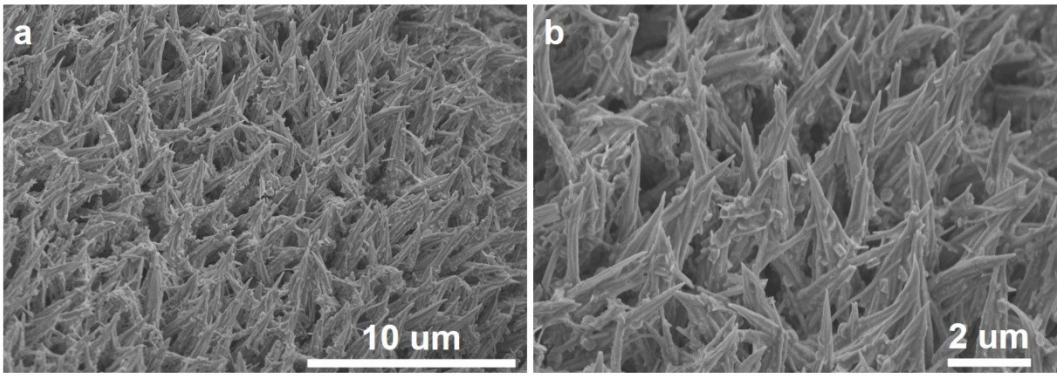

Fig. S16. The SEM images of NiCoP electrocatalyst after consecutive runs.

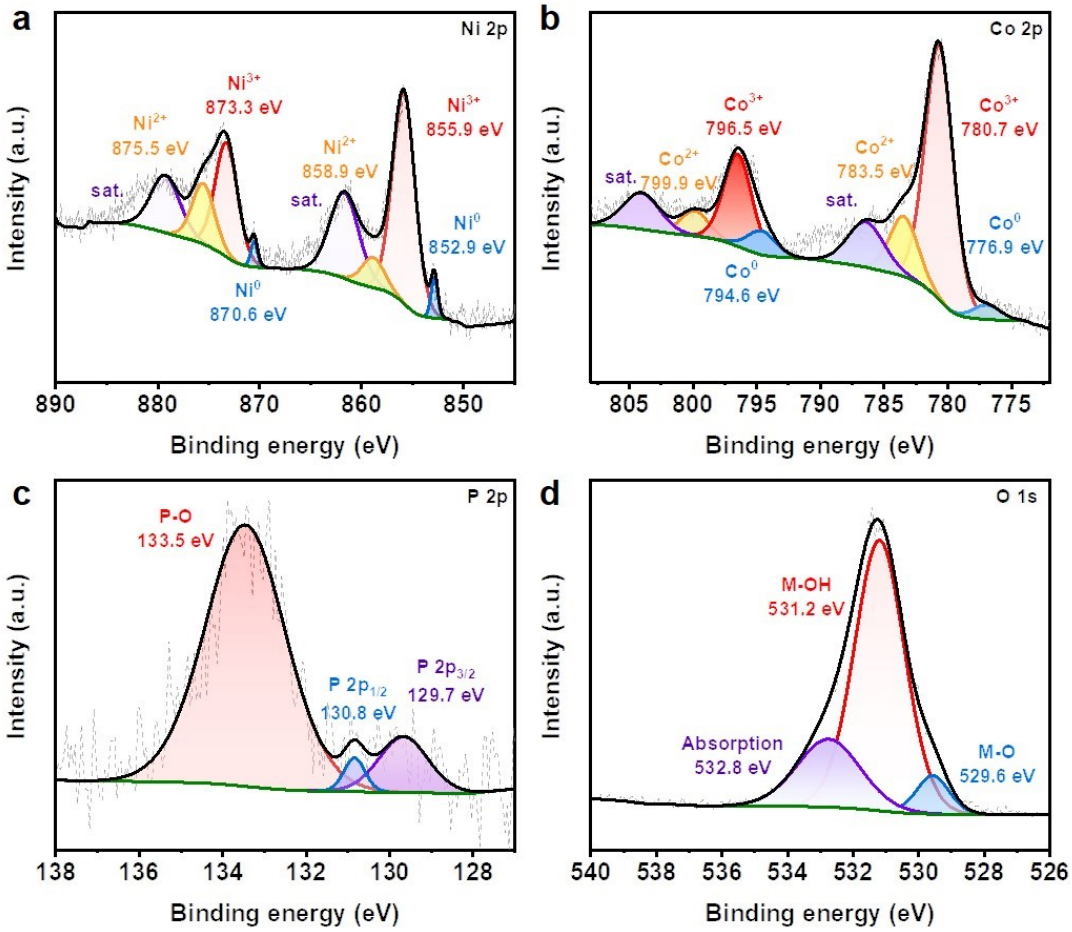

Fig. S17. XPS spectra of (a) Ni 2p, (b) Co 2p, (c) P 2p and (d) O 1s of NiCoP electrocatalyst after consecutive runs.

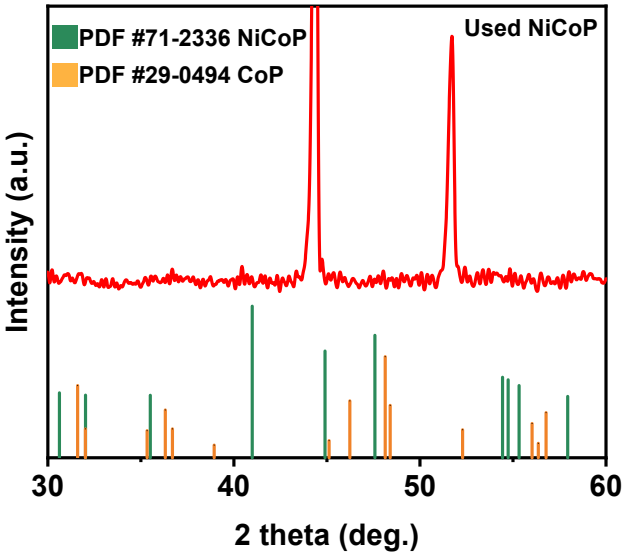

Fig. S18. XRD pattern of NiCoP after XOR.

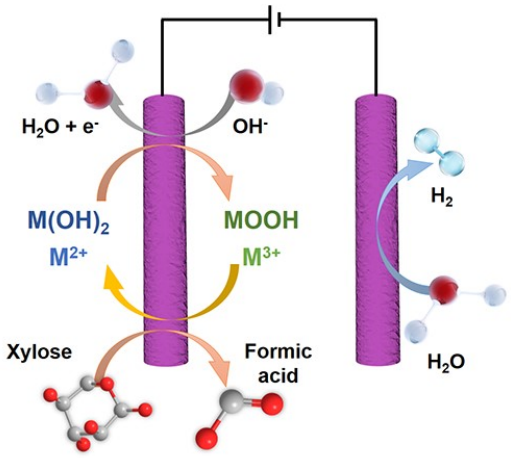

Fig. S19. The schematic of the reversible redox cycles of Ni^{2+}/Ni^{3+} and Co^{2+}/Co^{3+} during XOR with HER.

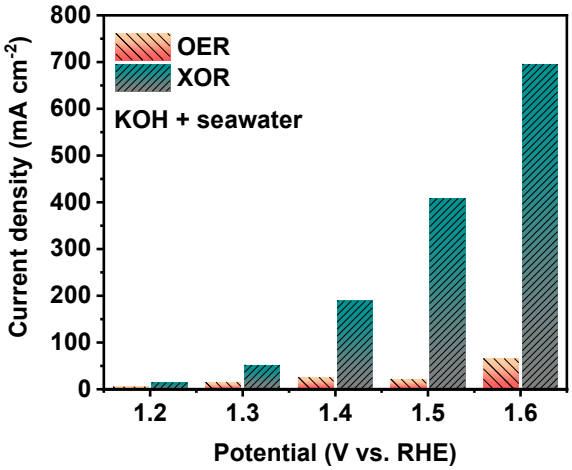

Fig. S20. The corresponding current densities at various potentials with (green bars) and without (orange bars) 100 mM xylose in 1.0 M KOH seawater.

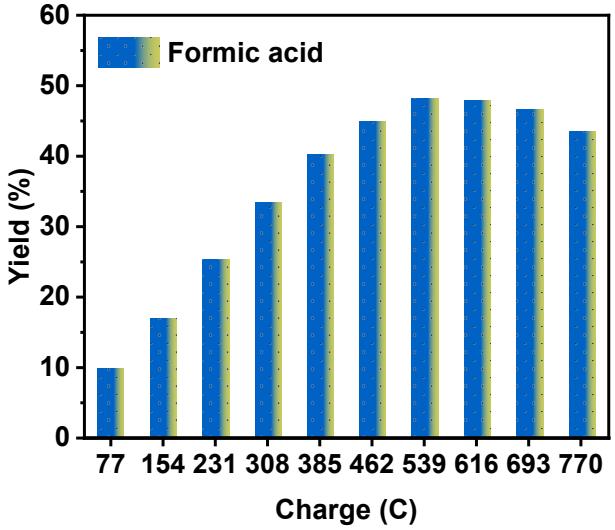

Fig. S21. The yield of FA from xylose after passing different charges at 1.52 V (*vs*. RHE) in alkaline seawater.

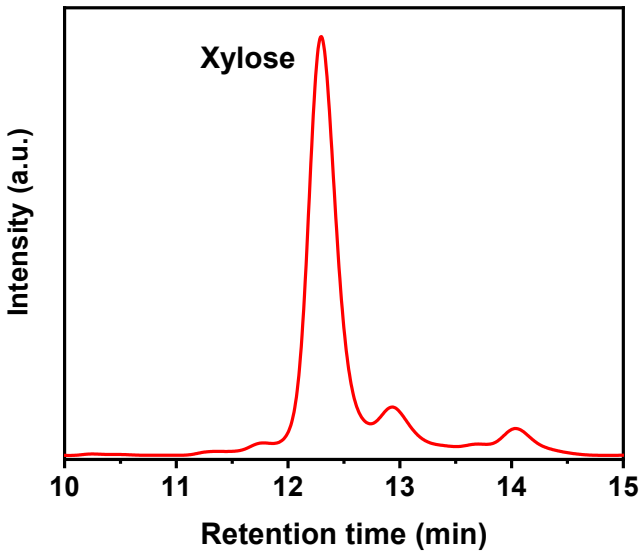

Fig. S22. HPLC traces of XOR after passing 540 C charges at 1.52 V (*vs.* RHE) in alkaline seawater.

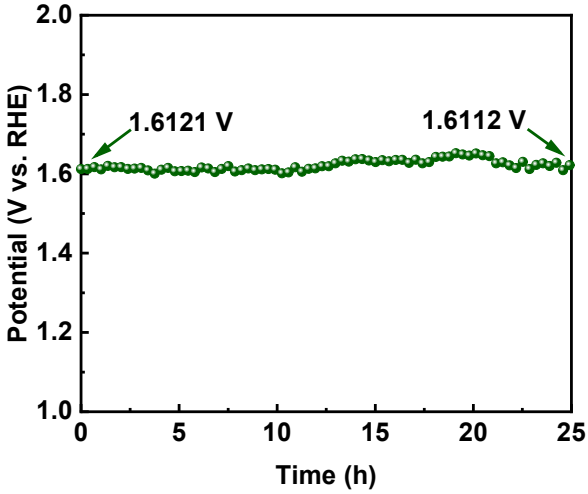

Fig. S23. Chronopotentiometry curve for NiCoP conducted at the current density of 50 mA cm^{-2} in alkaline seawater with 100 mM xylose.

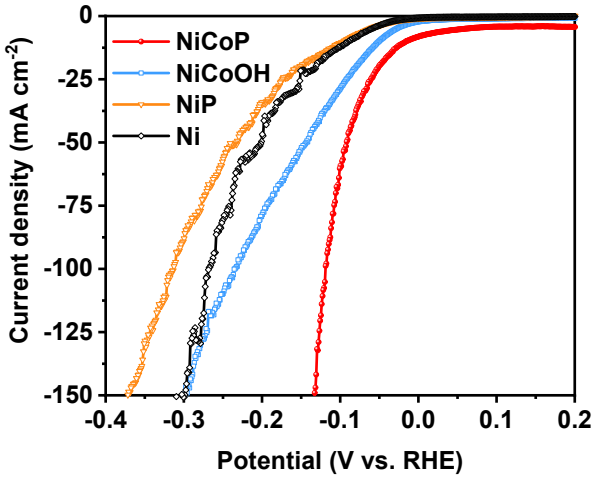

Fig. S24. LSV curves of different electrocatalysts in 1.0 M KOH.

The NiCoP electrocatalyst requires an overpotential of only 119 mV to drive the current intensity of 100 mA cm^{-2}, much lower than that of NiCoOH (201.6 mV), NiP (312.6 mV) and NF (268.6 mV).

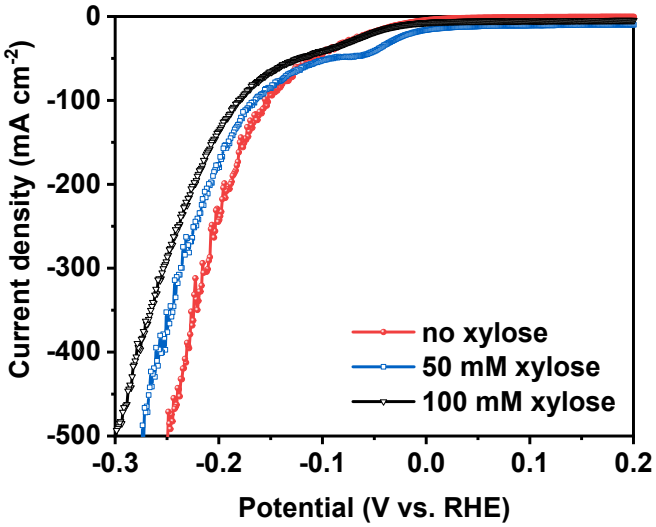

Fig. S25. LSV curves of different electrocatalysts in 1.0 M KOH with different concentrations of xylose.

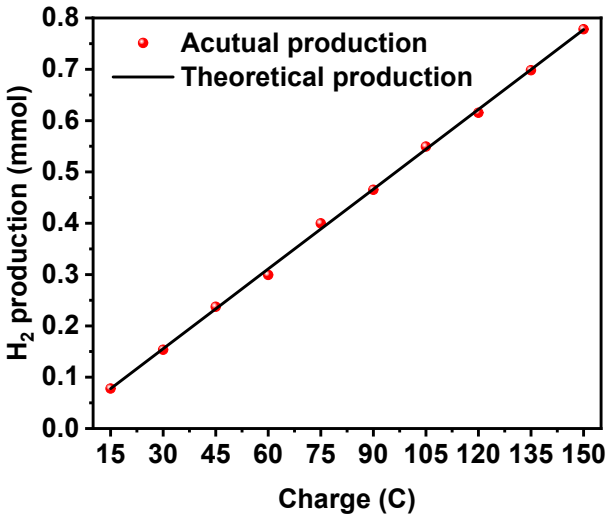

Fig. S26. Actual H_2 production compared with theoretically calculated H_2 production.

Table S1 Comparison of our catalyst with the reported catalyst for organic chemicals electrooxidation.

Electrocatalyst	Electrolyte	Potential (V *vs*. RHE)	j (mA cm^{-2})	Ref.
NiCoP-NF	1.0 M KOH + 0.1 M xylose	1.29	100	This work
$NiFeO_x$-NF	1.0 M KOH + 0.1 M glucose	1.30	87.6	[1]
CoFeCr LDH-NF	1.0 M KOH + 0.33 M urea	1.305	10	[2]
NiMoO-Ar-NF	1.0 M KOH + 0.5 M urea	1.42	100	[3]
Ni_2P-UNMs-NF	1.0 M KOH + 0.125 M benzylamine	1.34	10	[4]
Ni_3S_2-MoS_2-NF	1.0 M KOH + 0.02 M 5-hydroxymethylfurfural	1.33	50	[5]
O-NiMoP-NF	1.0 M KOH + 0.5 M urea	1.41	100	[6]
$Ni(OH)_2$-NF	1.0 M KOH + 0.5 M MeOH	1.36	100	[7]
NiFeCo LDH-NF	1.0 M KOH + 0.33 M urea	1.39	100	[8]
Ni_2P/Fe_2P-NF	1.0 M KOH + 0.5 M urea	1.36	10	[9]

Table S2 Co and P contents of NiCoP measured by ICP OES.

Sample	Element（wt%）	
	Co	P
Fresh	12.81	6.86
Used	11.14	2.78

Table S3 Comparison of our catalyst with the reported catalyst for HER.

Catalyst	η_{100}	Reference
NiCoP-NF	119	This work
$NiFeN_x$-NF	104	[10]
NF@NM-NP	164	[11]
Cu_2S/NF	289	[12]
Ni_2P-Fe_2P/NF	225	[13]
Fe-Ni_3S_2/NF	232	[14]
MoS_2–Ni_3S_2 HNRs/NF	191	[15]
Ni_3N-VN/NF	218	[16]
LDH-NiSe/NF	276	[17]
$CoMoO_4$ NWA/Ti	243	[18]

References

1 W.-J. Liu, Z. Xu, D. Zhao, X.-Q. Pan, H.-C. Li, X. Hu, Z.-Y. Fan, W.-K. Wang, G.-H. Zhao and S. Jin, *Nat. Commun.*, 2020, **11**, 265.

2 Z. Wang, W. Liu, Y. Hu, M. Guan, L. Xu, H. Li, J. Bao and H. Li, *Appl. Catal. B-Enivron.*, 2020, **272**, 118959.

3 Z.-Y. Yu, C.-C. Lang, M.-R. Gao, Y. Chen, Q.-Q. Fu, Y. Duan and S.-H. Yu, *Energ. Environ. Sci.*, 2018, **11**, 1890-1897.

4 Y. Ding, B.-Q. Miao, S.-N. Li, Y.-C. Jiang, Y.-Y. Liu, H.-C. Yao and Y. Chen, *Appl. Catal. B-Enivron.*, 2020, **268**, 118393.

5 S. Yang, Y. Guo, Y. Zhao, L. Zhang, H. Shen, J. Wang, J. Li, C. Wu, W. Wang, Y. Cao, S. Zhuo, Q. Zhang and H. Zhang, *Small*, 2022, **18**, 2201306.

6 H. Jiang, M. Sun, S. Wu, B. Huang, C.-S. Lee and W. Zhang, *Adv. Funct. Mater.*, 2021, **31**, 2104951.

7 J. Hao, J. Liu, D. Wu, M. Chen, Y. Liang, Q. Wang, L. Wang, X.-Z. Fu and J.-L. Luo, *Appl. Catal. B-Enivron.*, 2021, **281**, 119510.

8 P. Babar, A. Lokhande, V. Karade, B. Pawar, M. G. Gang, S. Pawar and J. H. Kim, *ACS Sustain. Chem. Eng.*, 2019, **7**, 10035-10043.

9 L. Yan, Y. Sun, E. Hu, J. Ning, Y. Zhong, Z. Zhang and Y. Hu, *J. Colloid Interf. Sci.*, 2019, **541**, 279-286.

10 W. Liu, Z. Xu, D. Zhao, X. Pan, H. Li, X. Hu, Z. Fan, W. Wang, G. Zhao and S. Jin, *Nat. Commun.*, 2020, **11**, 1-11.

11 P. Yang, M. Ren, C. Jin and H. Xing, *J. Electrochem. Soc.*, 2022, **169**, 046511.

12 T. Marimuthu, R. Yuvakkumar, P. S. Kumar, G. Ravi, X. Xu, D. Velauthapillai and N. V. Dai Viet, *Int. J. Hydrogen Energy*, 2022, **47**, 30819-30829.

13 L. Wu, L. Yu, F. Zhang, B. McElhenny, D. Luo, A. Karim, S. Chen and Z. Ren, *Adv. Funct. Mater.*, 2021, **31**, 2006484.

14 G. Zhang, Y. Feng, W. Lu, D. He, C. Wang, Y. Li, X. Wang and F. Cao, *ACS Catal.*, 2018, **8**, 5431-5441.

15 Y. Yang, K. Zhang, H. Lin, X. Li, H. C. Chan, L. Yang and Q. Gao, *ACS Catal.*, 2017, **7**, 2357-2366.

16 H. Yan, Y. Xie, A. Wu, Z. Cai, L. Wang, C. Tian, X. Zhang and H. Fu, *Adv. Mater.*, 2019, **31**, 1901174.

17 S. Dutta, A. Indra, Y. Feng, T. Song and U. Paik, *ACS Appl. Mater. Inter.*, 2017, **9**, 33766-33774.

18 J. Zhao, X. Ren, H. Ma, X. Sun, Y. Zhang, T. Yan, Q. Wei and D. Wu, *ACS Sustain. Chem. Eng.*, 2017, **5**, 10093-10098.